

---

# Modelling the Effects of Hearing Loss on Neural Coding in the Auditory Midbrain with Variational Conditioning

---

**Lloyd Pellatt**

Ear Institute  
University College London  
London,  
l.pellatt@ucl.ac.uk

**Fotios Drakopoulos**

Ear Institute  
University College London  
London,  
f.drakopoulos@ucl.ac.uk

**Shievanie Sabesan**

Ear Institute  
University College London  
London,  
s.sabesan@ucl.ac.uk

**Nicholas A. Lesica**

Ear Institute  
University College London  
London,  
n.lesica@ucl.ac.uk

## Abstract

The mapping from sound to neural activity that underlies hearing is highly non-linear. The first few stages of this mapping in the cochlea have been modelled successfully, initially with biophysical models built by hand and, more recently, with DNN models trained on datasets simulated by the biophysical models. Modelling the auditory brain has been a challenge because central auditory processing is too complex for models to be built by hand, and datasets for training DNN models directly have not been available. Recent work has taken advantage of large-scale high resolution neural recordings from the auditory midbrain to build a DNN model of normal hearing with great success. But this model assumes that auditory processing is the same in all brains, and therefore it cannot capture the widely varying effects of hearing loss.

We propose a novel variational-conditional model to learn to encode the space of hearing loss directly from recordings of neural activity in the auditory midbrain of healthy and noise exposed animals. With hearing loss parametrised by only 6 free parameters per animal, our model accurately predicts 62% of the explainable variance in neural responses from normal hearing animals and 68% for hearing impaired animals, within a few percentage points of state of the art animal specific models. We demonstrate that the model can be used to simulate realistic activity from out of sample animals by fitting only the learned conditioning parameters with Bayesian optimisation, achieving crossentropy loss within 2% of the optimum in 15-30 iterations. Including more animals in the training data slightly improved the performance on unseen animals. This model will enable future development of parametrised hearing loss compensation models trained to directly restore normal neural coding in hearing impaired brains, which can be quickly fitted for a new user by human in the loop optimisation.

# 1 Introduction

Computational models of neural responses to sound are widely used in the study of hearing and hearing loss [1]. Many current models focus on predicting responses in the cochlea and auditory nerve. These models can be parametrised to simulate different types of hearing loss, drawing on known biophysical causes of hearing loss such as inner/outer hair cell loss or cochlear synaptopathy [2], but with several important limitations. The engineered nature of these models means that they make assumptions about the effects of hearing loss, and that they are slow to compute and non-differentiable. In recent years deep learning has been used to approximate the non-linear mapping from sound to neural activity expressed by these analytically derived models in a more efficient and differentiable way [3, 4, 5, 6], but these models are trained on data generated by the original models, thereby inheriting their biases and assumptions. Additionally, even if models could provide perfect predictions of neural activity in the healthy and damaged cochlea, there are other important changes in the central auditory pathway due to brain plasticity that would not be accounted for [7, 8].

DNNs have also been used to model activity in the auditory cortex [9, 10]. However, these models only simulate activity with low spatial precision (fMRI data and field potentials respectively). Recently, a unique large-scale dataset of neural activity recordings has been collected from the inferior colliculus (IC) of a large number of normal hearing (NH) and noise exposed gerbils by Sabesan et al. [11]. This has enabled the development of deep learning models trained directly on real neural activity [11, 12]. These models are fast, differentiable and can incorporate all of the complex, non-linear properties of auditory processing up to the level of the midbrain. The limitation of this more direct approach is that it can only be used to simulate brain activity for specific animals from which there are existing recordings. While the models have been shown to accurately simulate both hearing impaired and normal hearing brain activity [11], this requires training a new model from scratch for every brain with different hearing status. Drakopoulos et al. [12] have shown that multi-branch DNNs trained to predict neural activity in the IC of multiple NH animals can capture shared dynamics across different brains. But while every healthy auditory system can be assumed to exhibit similar patterns of neural activity, every impaired system will exhibit its own unique distortions.

Drawing on conditional and ‘attribute-based’ generative models [13, 14, 15, 16], we propose a complete model of healthy and impaired neural coding in the auditory midbrain parametrised by a small set of parameters  $\psi$  which are directly learned from data and which represent a low dimensional encoding of the full spectrum of hearing loss. We show that the model learns to accurately simulate neural coding in a wide variety of hearing impaired and normal hearing brains without explicit assumptions as to the effects of hearing loss. We demonstrate that the space of conditioning parameters learned by the model is smooth and contains within it a latent description which can be used to accurately predict the neural activity of animals on which it was not trained. This constitutes the first model of the auditory midbrain which can simulate both healthy and impaired neural activity across a wide spectrum of hearing loss.

## 1.1 ICNet

The ICNet model proposed in [12] accurately simulates neural coding in the IC, represented as multi-unit activity (MUA) on each of 512 recording channels in 1.3 ms time bins. ICNet follows an encoder-decoder structure, where the convolutional encoder is used to extract salient features from the sound which are then interpreted by the decoder to predict the response recorded in an individual animal. The architecture of the sound encoder (which we also use) is given in figure 1b. The decoder is a single pointwise 1-D convolutional layer mapping the bottleneck to a  $512 \times 256 \times 5$  matrix, representing a five class categorical distribution over the number of spikes detected in each time bin. The model then samples from this predictive distribution to simulate neural activity.

This model architecture has been shown to reproduce the real MUA recorded from many individual animals with both normal hearing status and varying degrees of hearing loss with remarkable accuracy [11, 12]. A multi-branch architecture was shown to better model the neural responses of multiple normal hearing animals, using a shared sound encoder network and unique decoders for each animal [12]. Drakopoulos et al. demonstrate that a multi-branch model with a 64 channel bottleneck is enough to capture the shared latent dynamics of multiple individual NH animals and reproduce the resulting MUA with accuracy comparable to the single branch (i.e., animal specific) models [12].

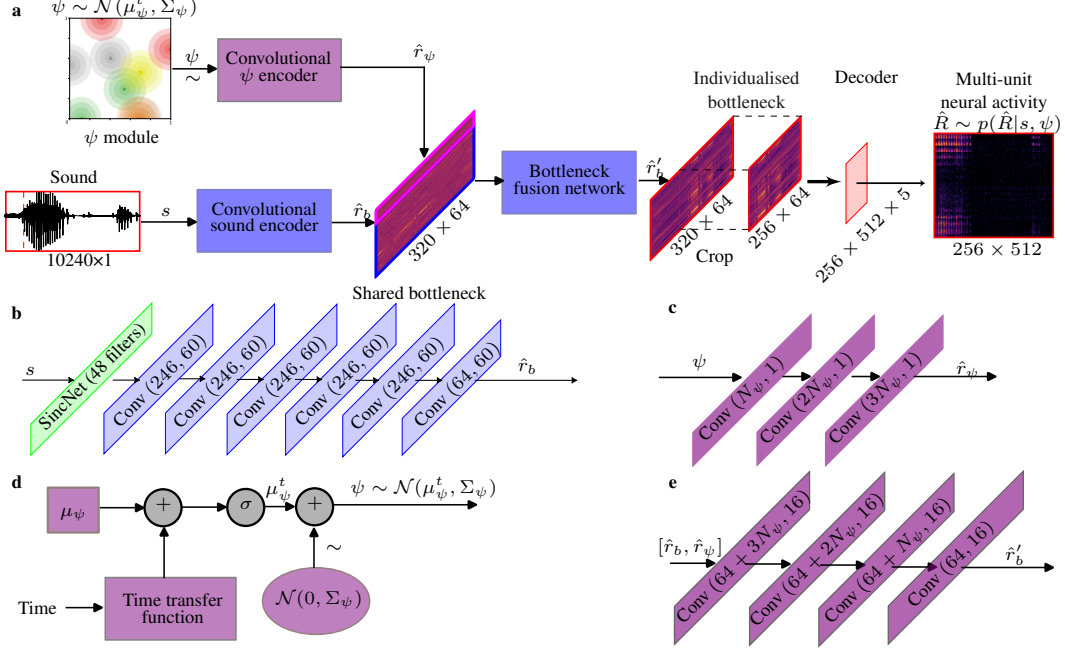


Figure 1: Part **a** shows the architecture of the variational-conditional model  $\psi$ -ICNet. An input sound is processed by a causal convolutional sound encoder **b**. The final convolutional layer produces a latent representation  $\hat{r}_b$  which encodes latent dynamics shared across all animals in the dataset. This shared representation is concatenated over the channel dimension with a small set of features  $\hat{r}_\psi$  extracted by the convolutional  $\psi$  encoder **c**. These features are decoded from an input sampled from a distribution over the conditioning variables  $\psi$  learned by the  $\psi$  module **d**. This distribution is a multivariate Gaussian with learned means  $\mu_\psi^t$  and covariance matrix  $\Sigma_\psi$ , which is diagonal. The  $\psi$  encoder **c** consists of three convolutional layers with increasing numbers of filters, producing a representation  $\hat{r}_\psi$  of size  $3N_\psi \times 320$  where  $N_\psi$  is the number of  $\psi$  parameters. The bottleneck fusion network **d** then combines the shared and animal-specific information with 4 convolutional layers containing progressively fewer kernels of size 16, reducing the dimensionality back to that of the original shared representation  $\hat{r}_b$ . This produces an individualised latent representation  $\hat{r}'_b$ , which is cropped to remove the context and passed through a shared simple decoder. The decoder produces a categorical probability distribution  $p(\hat{R}|s, \psi)$  over the number of spikes for each channel at each time bin, from which we sample to produce the simulated neural activity  $\hat{R}$ .

## 1.2 Conditional models

In [5], Bysted et al. propose a similar framework to our proposed conditional model, in which weights for a deep learning based model of the cochlea up to the level of inner hair cells are generated from an audiogram by a weight generating network. This differs from our work in two important ways. Firstly, the Bysted et al. model includes only the most peripheral stages of the auditory system, whereas ours reflects the processing that takes place in the cochlea, brainstem and midbrain. Also, our method learns the underlying structure of the space of hearing loss directly from the distribution of hearing impaired brains in the training dataset, rather than relying on audiometric thresholds to inform the parameter space. This is advantageous since audiometric thresholds have been shown to be inadequate descriptors of hearing loss, as illustrated most clearly by the prevalence of ‘hidden hearing loss’, a condition in which a patient exhibits impaired perception of complex sounds despite normal audiometric test results [17]. Any perceptual difficulties which are not reflected in audiometric measurements should nonetheless result in distorted or reduced neural activity in the IC.

## 2 Variational-conditional model

Figure 1 shows the general framework for our conditional model. We use the same sound encoder as the ICNet model to extract a shared 64 channel latent representation of the sound. This shared representation is then individualised by incorporating a set of learned conditioning parameters  $\psi$  which encode the differences between brains due to hearing loss. The  $\psi$  parameters are the only part of the model which is learned uniquely for a given animal—all other parameters in the model are shared between animals. The means  $\mu_\psi^t$  are dependent on the measurement time of the MUA according to the time degradation module described in appendix A, to account for the non-stationarity of the neural responses over time. Once the latent feature maps have been conditioned on the  $\psi$  parameters, we pass the individual representations  $\hat{r}_b'$  through a shared decoder which projects from the latent space to a 512 channel MUA representation.

In addition to the concatenative model illustrated in figure 1, we investigated whether including an attention mechanism in the model would improve our results. We applied cross attention [18] to the bottleneck responses using the processed  $\psi$  parameters as the ‘key’ and the bottleneck as the ‘query’ and ‘value’. The attention operation was performed over the channel dimension in the bottleneck. The processed  $\psi$  parameters are then concatenated to the appended bottleneck features and the rest of the architecture proceeds as in figure 1.

### 2.1 ABRNet

To test our hypothesis that learning conditioning parameters directly from the data can produce a conditioning space that works better than an equivalent approach using audiometric measurements, we implemented a variation of our model architecture where the learned means  $\mu_\psi$  of the conditioning variables are replaced by the auditory brainstem response (ABR) threshold measurements from each animal in response to tones at 1, 2, 4, 8, and 16kHz. These ABR thresholds constitute a description of the specific hearing loss profile of the animal comparable to an audiogram measured from a human listener, and therefore ABRNet should be able to learn to generate individualised responses to some degree. We did not add Gaussian noise to the ABR thresholds for this model. Otherwise the model architecture is the same as the  $\psi$ -ICNet architecture described in figure 1.

### 2.2 Loss function

We trained each model according to a loss function specified by:

$$\mathcal{L} = \alpha(\mathcal{L}_{CE}(q(R), p(\hat{R}))) + \alpha_{KL} D_{KL}(\mathcal{N}(\mu_\psi^t, \Sigma_\psi) || \mathcal{N}(\mu_\psi^t, \Sigma^*)) + \alpha_{ABR} \mathcal{L}_{ABR}, \quad (1)$$

where  $\alpha$  represents the overall learning rate,  $\mathcal{L}_{CE}$  is the crossentropy loss between the output of the model and a one-hot representation of the target MUA. The  $D_{KL}$  term is the KL divergence between the encoded  $\psi$  distributions and a target distribution with covariance matrix  $\Sigma^* = \frac{1}{N_A} \cdot \mathbb{I}$  where  $N_A$  is the number of animals, and  $\alpha_{KL}$  is a weighting coefficient.

In order to further encourage the model to cluster animals with similar hearing loss together in the  $\psi$  space, we additionally applied a small penalty  $\mathcal{L}_{ABR}$  in the first 10 epochs for encoding animals with similar ABR thresholds close together, given by

$$L_{abr} = w \sum_{i,j} A_{ij} e^{(-10 \frac{d_{ij}}{\bar{d}})}, \quad A_{ij} = \sqrt{\frac{1}{m} \sum_{k=1}^m (T_{ik} - T_{jk})^2}, \quad \bar{d} = \sqrt{\frac{n}{6} - \frac{7}{120}} \quad (2)$$

where  $m$  is the number of frequencies (1, 2, 4, 8, and 16 KHz) at which ABR thresholds were measured, and the sum is taken over all unique pairs  $(i, j)$  where  $i \neq j$ .  $d_{ij} = \frac{1}{n} \sum_{k=1}^n |\mu_{\psi,ik} - \mu_{\psi,jk}|$  is the mean absolute difference between learned means for animals  $i$  and  $j$  and  $A_{ij}$  is the RMSE between the ABR thresholds  $T$  of animals  $i$  and  $j$ . We scale the distances by  $\bar{d}$ , which gives the expected distance between two random points in a unit hypercube of dimension  $n$ , to account for the curse of dimensionality and ensure that the penalty is applied sensibly across different numbers of  $\psi$  parameters.



### 2.3 Hyperparameters

We trained each model using the Adam optimiser [19] for up to 120 epochs, stopping early if validation loss did not improve for 10 epochs in a row. We reduced the learning rate  $\alpha$  by half if the validation loss did not improve for 4 epochs in a row. The encoders for all models were initialised with weights from a multi-branch model trained on 12 NH animals, to speed up convergence.

We used a weighting of  $\alpha_{KL} = 10^{-3}$  for the KL divergence term, and defined a target covariance matrix  $\Sigma^* = \mathbf{I} \cdot \frac{1}{N_A}$ , where  $N_A$  is the number of animals in the training data. This ensures some overlap in the distributions between different animals. We used a weighting of  $\alpha_{ABR} = 0.02$  for the first 10 epochs and  $\alpha_{ABR} = 0$  afterwards.

For the sound encoder, we trained 48 bandpass filters in the initial SincNet layer and 246 kernels of size 60 in each strided convolutional layer, and 64 kernels of size 60 for the final layer to produce a shared latent representation of 64 channels. We used either 3 or 6  $\psi$  parameters, and chose the number of pointwise filters in the  $\psi$  encoder accordingly as described in figure 1 to produce a latent representation  $\hat{r}_\psi$  with  $3N_\psi$  channels. For the bottleneck fusion network, we used filters of size 16.

### 2.4 Performance metrics

Since the neural activity recorded from the IC is noisy, we need to determine how well our models capture the repeatable signal in the data. To measure this we take two recordings  $R_1$  and  $R_2$  of MUA produced from identical sounds, we predict two responses  $\hat{R}_1$  and  $\hat{R}_2$  to the same sound, and we compute the fraction of explainable variance explained (FEVE), weighted by the cross-trial covariance of each channel, given by:

$$\text{FEVE} = \frac{1}{M} \sum_{i=1}^M w_i \cdot \left( 1 - \frac{\frac{1}{2T} \left( \sum_{t=1}^T (R_t^{1,i} - \mathbb{E}_C[\hat{R}_t^{1,i}])^2 + \sum_{t=1}^T (R_t^{2,i} - \mathbb{E}_C[\hat{R}_t^{2,i}])^2 \right) - \sigma_{noise,i}^2}{\frac{1}{2}(\text{Var}(R_t^{1,i}) + \text{Var}(R_t^{2,i})) - \sigma_{noise,i}^2} \right) \quad (3)$$

where  $w_i = \text{Cov}(y_t^{1,i}, y_t^{2,i})$  is the covariance of channel  $i$  between the two trials in the recorded data,  $E_c$  is the expectation over spike counts of the model output  $p(\hat{R}|s, \psi)$  for  $\psi$ -ICNet,  $\sigma_{noise}^2 = \frac{1}{2} \text{Var}(R_t^{1,i} - R_t^{2,i})$  is a measure of the background noise level in the MUA, and  $M$  and  $T$  are the size of the channel and time dimension respectively. 100% FEVE would mean that all of the consistent information in the original data  $(R_1, R_2)$  is present in the generated data  $(\hat{R}_1, \hat{R}_2)$ .

We also computed the covariance weighted KL divergence between the normalised spike count histograms of the true and predicted MUA, given by

$$KL = \sum_{i=1}^M w_i \cdot \frac{1}{2} (KL(H_1^i || H_2^i) + KL(H_2^i || H_1^i)), \quad H^i = \frac{\sum_{t=1}^T \mathbb{I}(R_t^i = l_i)}{\sum_{j=1}^L \sum_{t=1}^T \mathbb{I}(R_t^i = l_j)}. \quad (4)$$

Zero weighted KL divergence would mean that the distribution of spikes in the generated data is identical to the distribution in the recorded data.

### 2.5 Computational resources

Each training run of the multi-animal models described in this paper required around 10-20 GPU hours of training time on a single RTX 4090 GPU with 24GB VRAM, depending on early stopping, while the single animal models required 3-5 hours of training on a single GPU. All experiments were performed locally on a GPU server with 4 RTX 4090 GPUs and 256GB of system memory. In total, experiments reported in this paper used around 300-500 GPU hours of compute. We estimate that the research project so far has consumed several thousand GPU hours including preliminary experiments and additional experiments whose results are not reported in this paper.

Model	FEVE		KL Divergence / $10^{-3}$	
	NH	HI	NH	HI
ICNet (single)	$66.9 \pm 13.5$	$70.7 \pm 11.3$	$8.39 \pm 2.11$	$10.4 \pm 3.47$
ABRNet	$-5.60 \pm 4.34$	$-3.72 \pm 9.91$	$-0.36 \pm 2.54$	$-0.35 \pm 5.58$
Concatenative - 3 $\psi$	$-7.23 \pm 4.82$	$-3.47 \pm 9.70$	$-0.98 \pm 2.50$	$-1.00 \pm 4.21$
Concatenative - 6 $\psi$	$-5.31 \pm 5.12$	$-2.14 \pm 7.30$	$-1.14 \pm 2.72$	$-1.26 \pm 4.13$
Attention - 6 $\psi$	$-5.60 \pm 3.38$	$-3.20 \pm 10.8$	$0.49 \pm 2.94$	$0.13 \pm 5.40$

Table 1: Table showing the relative performance of each of our  $\psi$  models compared to the animal specific ICNet models, in terms of the covariance weighted FEVE and KL divergence as explained in section 2.4. We give the median pairwise difference and median absolute deviation between the single branch model and our models for each metric over all sounds, split between NH and HI animals.

### 3 Dataset collection and preparation

We trained our models on a dataset of MUA recorded from 9 gerbils, 3 of which had normal hearing and 6 of which were noise exposed with symmetric hearing impairment (determined by comparing ABR thresholds across ears), according to the procedure outlined in [11]. For each animal, there is a dataset of 512 channel MUA, where each channel represents the spiking activity of a small group of neurons in the IC. Audio data was recorded at a sampling frequency of 24.4 kHz. MUA was extracted from neural activity recorded at 20 KHz and resampled a frequency of 762.9395 Hz, giving our model a temporal precision of 1.3 ms. To prepare the data for training, we segmented the audio and MUA into frames of 0.33 seconds. We included context of 2048 samples (0.08 seconds) at the beginning of each frame of audio to avoid padding with synthetic data, which was cropped from the features extracted by the the convolutional layers.

The training dataset contained 7.8 hrs of data, consisting of a mixture of speech, processed speech, speech in noise, music and dynamic ripples [12], split 90:10 between training and validation. We tested the models using a variety of 30 s segments of sounds from the same classes but from different sources (e.g., speech corpora).

#### 3.1 Alignment between brains

Even two animals with normal hearing will produce neural responses which differ in subtle ways, due to differences in the spatial organisation of information in the IC. Therefore, to ensure that the parameter space learned by our model primarily encodes differences related to hearing loss, rather than correcting this misalignment, and to allow us to use a shared decoder, we must remove this source of variability from the dataset before training the model. To accomplish this, we used optimal transport to find a permutation of the channels of each brain recording that minimised the Wasserstein distance to a common NH reference animal.

### 4 Comparison against single branch model

Table 1 reports the median FEVE and KL divergence of the single branch ICNets on the test set, and the median pairwise difference to the score of the single branch model  $\pm$  the median absolute deviation (MAD) over all sounds and animals for the other models. We used the median and MAD since there were several outliers, mainly from the speech in noise and ripples sounds. The single branch model generally performs best in terms of FEVE for any given animal, but the 6 parameter concatenative  $\psi$ -ICNet comes very close for hearing impaired animals, and matches or outperforms the single branch model in terms of KL divergence. ABRNet performs worse than all other models for hearing impaired animals and worse than the 6 parameter concatenative model for NH animals. Our implementation of cross-attention does not seem to have improved the performance of  $\psi$ -ICNet. Figure 2 provides visual examples of the responses predicted by the  $\psi$ -ICNet model compared to the true responses and the predictions of the single branch models, for different animals and sounds.

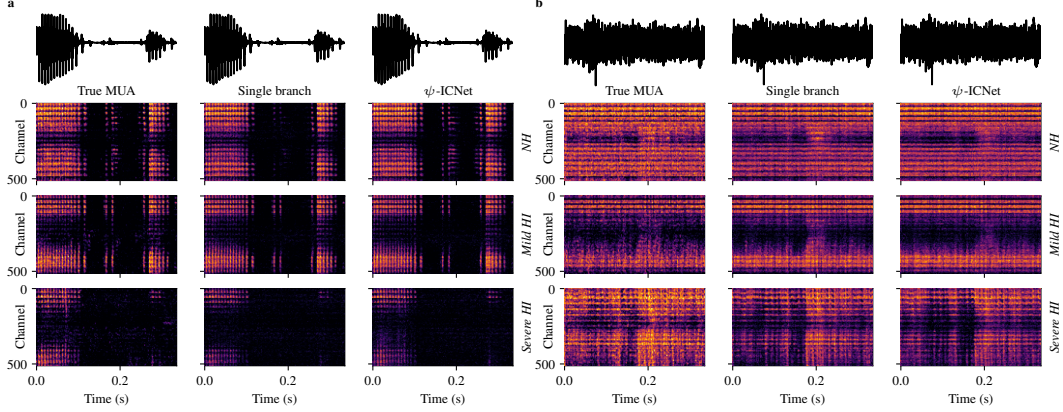


Figure 2: Figure showing comparisons of  $\psi$ -ICNet to the single branch ICNet models. **a** and **b** show examples of the MUA predicted by the model when given audio stimuli corresponding to clean speech and music respectively. The left column shows the real MUA recorded from three animals—one NH, one with mild hearing loss and one with severe hearing loss. The middle and rightmost columns show the MUA predicted by the single branch model and the  $\psi$ -ICNet model respectively.

## 5 Generating data from unseen animals

We used a simple Bayesian optimisation routine to search through the  $\psi$  space of the trained concatenative models with 3 and 6  $\psi$  parameters to find the optimal conditioning parameters  $\psi^*$  for four animals (of which two were included in the training set, and two were not). We initialised the Gaussian process with 4, 8 or 16 evenly spaced random samples drawn from a Sobol sequence. At each step we evaluated the model’s performance on a 30 minute subset of the training data consisting of 15 seconds from each sound in the training data which was collected in the first 2 hours of the experiment, so as to keep the effects of time degradation to a minimum (time degradation is encoded into the  $\psi$  space as described in the appendix A). The Bayesian optimisation routine was stopped when it found a candidate for  $\psi^*$  which produced a loss within 2% of the target loss. The target loss was taken as the value of the loss achieved using the learned means of the  $\psi$  distributions.

While we found that these models could converge quickly to a value of  $\psi$  close to the optimum for both in-sample and out of sample animals, performance on out of sample animals is significantly worse than for in-sample animals. This may simply be due to the low number of animals included in the space, so we also trained the 6 parameter model on data from 10 normal hearing and 10 symmetric hearing impaired animals. We used the same hyperparameters except for the initial learning rate, which we set lower at  $1 \times 10^{-4}$ . We tested the 9 animal and 20 animal versions on 4 held out animals which were not seen by either model, and 4 in-sample animals which were included in training data for both models. We used a subset of the test data which was recorded in the first few hours of the experiment for the evaluation, consisting of one 30 second sound from each sound class. Results from these evaluations are reported in figures 3l to o.

### 5.1 Results

As shown in figures 3a and 3b, we found that using Bayesian optimisation we could generally converge to a value of  $\psi$  which achieved within 2% of the minimum cross-entropy loss between the output of the model and the real response. For in-sample animals this was possible within 10-20 iterations for the 3 parameter model, while the 6 parameter model required 15-35 iterations.

Figures 3c to j show the results of our Bayesian optimisation over the  $\psi$  space of the 3 and 6 parameter concatenative models. The optimal  $\psi^*$  values found by Bayesian optimisation (the black crosses) are clustered around the learned value of  $\psi$  for each animal (the red stars), even for the severely hearing impaired animal in figure 3e for which only a small area of the  $\psi$  space produces a good loss.

The 3 parameter model learns  $\psi$  parameters with a smoothly varying loss surface for both HI and NH animals, in and out of sample. In particular, figures 3c and 3d, representing in/out of sample

NH animals, have very similar loss surfaces. There is also a clear contrast between these normal hearing loss surfaces and the loss surfaces for the hearing impaired animals shown in figures 3e and 3f. Figures 3g to j show that the same holds even for models with six  $\psi$  parameters, although the results are harder to interpret since we have projected six dimensions on to two.

Finally, figure 3k shows real and simulated MUA for 4 unseen animals with varying hearing status generated by the trained model using  $\psi^*$  found by Bayesian optimisation. As shown in figures 3l to o, we found that training the 6 parameter model with more animals improved the median FEVE score to 26.9% from 7.8% on unseen animals, while slightly degrading the median FEVE on in-sample animals from 55.6% to 50.7%.

## 6 Discussion and limitations

Although we demonstrated that we are able to learn a small set of control parameters which lead to a smoothly varying expression of hearing loss over a range of animals, the single branch ICNet architecture is still slightly better at predicting the responses of a specific animal, outperforming our model in terms of FEVE over most sounds. Inclusion of an attention mechanism did not improve the performance of  $\psi$ -ICNet, nor did several other modifications we tried during development.

We found that when evaluated on 4 animals which were included in the training set of both models, the performance was slightly degraded, as shown in figures 3l and n. This could indicate that more than 6 dimensions are needed for our model to capture the full spectrum of hearing loss described by these 20 animals —perhaps because the true dimensionality of the space of hearing loss is larger, or because the constraint on the scale of the  $\psi$  distributions is too strict, not allowing the model to encode a fine enough structure in the latent space. It could also be an indication that the model is learning a more generic representation with less non-hearing-related idiosyncrasies of specific animals, leading to a convergence between the performance on seen and unseen animals. Objective performance on unseen animals was still worse than in-sample animals for both models.

As shown in figure 3k, the simulated MUA qualitatively resembles the true MUA for unseen animals in the speech in quiet regime to a large degree. Where there are differences, they may be related to misalignment of recordings between animals as much as an inability to capture hearing loss.

## 7 Conclusion

We have described a novel variational-conditional model for parametrising hearing loss which can learn to generate individualised simulations of activity in the auditory midbrain by learning variational conditioning parameters directly from the data. We have shown that this model performs comparably to existing deep learning models trained from scratch on specific brains with varying hearing ability, and that by learning conditioning parameters directly from the data we achieve better performance than an equivalent architecture conditioned on measured ABR thresholds for each animal.

We have also demonstrated that we can quickly (within 15-30 iterations) optimise the model for a new brain, fitting only the conditioning  $\psi$  parameters with Bayesian optimisation, and that the space of  $\psi$  parameters encodes a smoothly varying spectrum of hearing loss. We showed that using these fitted  $\psi$  parameters, we can generate MUA for unseen animals which qualitatively resembles the MUA of the real animal, and which accurately predicts 25+% of the explainable variance in the neural responses. Although this is far off the performance of animal specific models, we predict that including more animals in the training data will allow us to further improve the performance.

### 7.1 Future Work and Applications

Core sound processing in current hearing aids is limited to frequency dependent amplification and compression, but we know that the real effects of hearing loss are much more complex than loss of sensitivity to certain frequencies and shifted dynamic range [11]. Amplification may restore audibility in situations where relevant audio stimuli are too quiet to hear, but it cannot restore lost intelligibility caused by more complex distortions of the neural code. One approach to developing hearing aids beyond the current state of the art is to use auditory models of NH and HI brains to develop sound processing algorithms which can directly correct the distorted neural code [20].

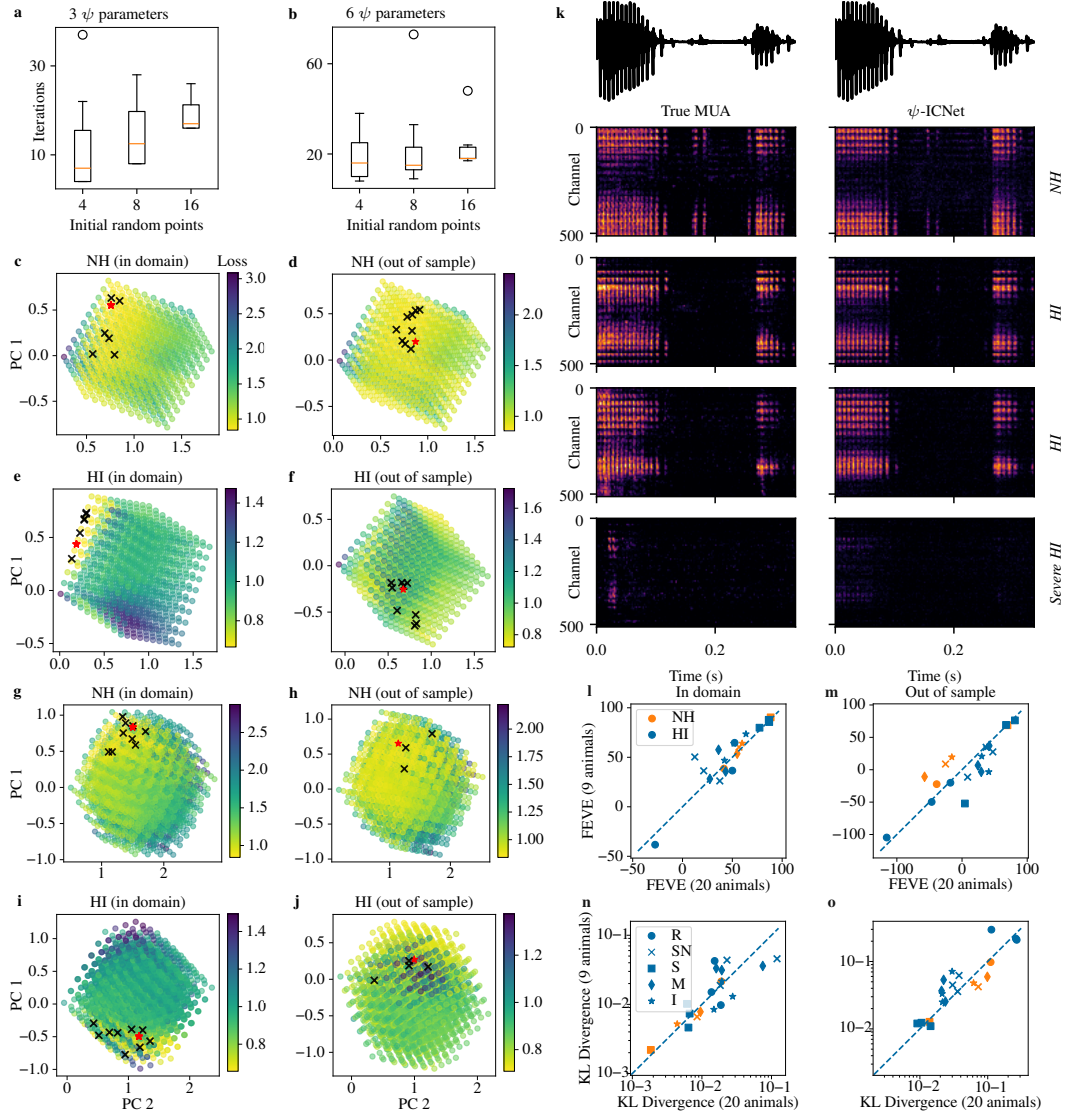


Figure 3: Figures **a** and **b** show the number of iterations required to converge to the target loss (see section 5) when starting with different numbers of random samples, for the 3 and 6 parameter concatenative model. Subfigures **c** to **f** show the loss surface over a 2D projection of 1000 evenly spaced points in the  $\psi$  space for 4 animals —two NH and two HI, two in-sample and two out of sample —in the 3 parameter  $\psi$ -ICNet. The colour of each point represents the loss obtained by generating MUA from the trained model with  $\psi$  fixed to the given values. The black crosses represent the values of  $\psi^*$  arrived at by the Bayesian optimisation routine over repeated runs, and the target  $\psi$  value learned during training (or the best point found in a grid search if the animal is unseen) is marked by a red star. Subfigures **g** to **j** show the same plots for the for the 6 parameter model, for which 4096 points in the  $\psi$  space were evaluated in the grid search. Figure **k** shows real (left) and simulated (right) MUA in response to a segment of speech for a model trained on 20 animals, 10 NH and 10 HI, when fitted to 4 different unseen animals with varying hearing status. The hearing status of the animal is indicated on the right of the row. Figures **l** and **m** show the relative FEVE of the 9 animal vs the 20 animal model for in-sample and out of sample animals, with NH animals highlighted in orange and HI animals in blue. Figures **n** and **o** show the relative KL divergence. Different markers represent different sound classes. Key: R = ripples, SN = speech in noise, S = clean speech, M = music, I = single instruments.

Following this approach, Drakopoulos et al. [6] and Leer et al. [21] have trained DNN-based hearing compensation strategies on the outputs of DNN-based models of the NH and HI auditory system. This has recently led to the first subjective evaluations of deep-learning based hearing compensation in listening tests with hearing impaired listeners [21], in which DNN-based hearing loss compensation outperforms state of the art hearing aids across all measures.

Compared to other state of the art DNN-based models of the auditory system, our model has several advantages when used for this purpose —first, we simulate activity in the midbrain rather than the ear, and second, our models are trained directly on recorded data rather than data simulated by engineered models. A parametrised hearing compensation model could be trained to correct distortions in the neural code for a wide range of hearing loss by sampling from the space of hearing loss which we learn during training. This would allow development of a hearing aid with a small set of control parameters which are directly related to the effects of hearing loss on the neural code, which could then be quickly fitted to a new listener by human in the loop optimisation. The success of our model in generating neural activity for brains with unseen hearing loss profiles by searching over the  $\psi$  space gives us confidence in this approach.

## References

- [1] Osses Vecchi, Alejandro, Varnet, Léo, Carney, Laurel H., Dau, Torsten, Bruce, Ian C., Verhulst, Sarah, and Majdak, Piotr, “A comparative study of eight human auditory models of monaural processing,” *Acta Acustica*, vol. 6, p. 17, 2022.
- [2] S. Verhulst, A. Altoe, and V. Vasilkov, “Computational modeling of the human auditory periphery: Auditory-nerve responses, evoked potentials and hearing loss,” *Hearing research*, vol. 360, pp. 55–75, 2018.
- [3] D. Baby, A. Van Den Broucke, and S. Verhulst, “A convolutional neural-network model of human cochlear mechanics and filter tuning for real-time applications,” *Nature machine intelligence*, vol. 3, no. 2, pp. 134–143, 2021.
- [4] A. Nagathil and I. C. Bruce, “Wavenet-based approximation of a cochlear filtering and hair cell transduction model,” *The Journal of the Acoustical Society of America*, vol. 154, no. 1, pp. 191–202, 2023.
- [5] P. A. L. Bysted, J. Jensen, Z.-H. Tan, J. Østergaard, and L. Bramsløw, “A parameter-conditional neural network framework for modelling parameterized auditory models,” in *Proceedings of the Euroregio/BNAM Joint Acoustics Conference*, pp. 307–316, 2022.
- [6] F. Drakopoulos and S. Verhulst, “A neural-network framework for the design of individualised hearing-loss compensation,” *IEEE/ACM Transactions on Audio, Speech, and Language Processing*, vol. 31, pp. 2395–2409, 2023.
- [7] J. J. Nelson and K. Chen, “The relationship of tinnitus, hyperacusis, and hearing loss,” *Ear, nose & throat journal*, vol. 83, no. 7, pp. 472–476, 2004.
- [8] B. D. Auerbach, P. V. Rodrigues, and R. J. Salvi, “Central gain control in tinnitus and hyperacusis,” *Frontiers in neurology*, vol. 5, p. 206, 2014.
- [9] A. J. Kell, D. L. Yamins, E. N. Shook, S. V. Norman-Haignere, and J. H. McDermott, “A task-optimized neural network replicates human auditory behavior, predicts brain responses, and reveals a cortical processing hierarchy,” *Neuron*, vol. 98, no. 3, pp. 630–644, 2018.
- [10] M. Keshishian, H. Akbari, B. Khalighinejad, J. L. Herrero, A. D. Mehta, and N. Mesgarani, “Estimating and interpreting nonlinear receptive field of sensory neural responses with deep neural network models,” *eLife*, vol. 9, p. e53445, jun 2020.
- [11] S. Sabesan, A. Fragner, C. Bench, F. Drakopoulos, and N. A. Lesica, “Large-scale electrophysiology and deep learning reveal distorted neural signal dynamics after hearing loss,” *eLife*, vol. 12, p. e85108, may 2023.
- [12] F. Drakopoulos, S. Sabesan, Y. Xia, A. Fragner, and N. A. Lesica, “Modeling neural coding in the auditory midbrain with high resolution and accuracy,” *bioRxiv*, 2024.
- [13] G. Lample, N. Zeghidour, N. Usunier, A. Bordes, L. Denoyer, and M. Ranzato, “Fader networks: Manipulating images by sliding attributes,” *Advances in neural information processing systems*, vol. 30, 2017.

- [14] O. Ivanov, M. Figurnov, and D. Vetrov, “Variational autoencoder with arbitrary conditioning,” in *International Conference on Learning Representations*, 2019.
- [15] L. Kawai, P. Esling, and T. Harada, “Attributes-aware deep music transformation.,” in *ISMIR*, pp. 670–677, 2020.
- [16] Y. Zong and J. Reiss, “Learning control of neural sound effects synthesis from physically inspired models,” in *ICASSP 2025-2025 IEEE International Conference on Acoustics, Speech and Signal Processing (ICASSP)*, pp. 1–5, IEEE, 2025.
- [17] C. J. Plack, D. Barker, and G. Prendergast, “Perceptual consequences of “hidden” hearing loss,” *Trends in hearing*, vol. 18, 2014.
- [18] A. Vaswani, N. Shazeer, N. Parmar, J. Uszkoreit, L. Jones, A. N. Gomez, Ł. Kaiser, and I. Polosukhin, “Attention is all you need,” *Advances in neural information processing systems*, vol. 30, 2017.
- [19] D. P. Kingma and J. Ba, “Adam: A method for stochastic optimization,” in *3rd International Conference on Learning Representations, ICLR 2015, San Diego, CA, USA, May 7-9, 2015, Conference Track Proceedings* (Y. Bengio and Y. LeCun, eds.), 2015.
- [20] J. Bondy, S. Becker, I. Bruce, L. Trainor, and S. Haykin, “A novel signal-processing strategy for hearing-aid design: neurocompensation,” *Signal Processing*, vol. 84, no. 7, pp. 1239–1253, 2004.
- [21] P. Leer, J. Jensen, L. H. Carney, Z.-H. Tan, J. Østergaard, and L. Bramsløw, “Hearing-loss compensation using deep neural networks: A framework and results from a listening test,” *IEEE Transactions on Audio, Speech and Language Processing*, 2025.

## A Modelling changes in neural responses over time

To better model the neural activity over the whole duration of the experiment while also capturing elements of the degradation over time of each animal which mimic an increase in the severity of hearing loss, we apply a modifier to the mean of the learned  $\psi$  distributions for each animal which is proportional to the time elapsed since the beginning of the experiment, which we give as an additional input  $t$  to the model where  $t$  is approximately the time elapsed in hours divided by 10. The effect of time on the neural activity of a given animal is assumed to conform to these specifications, informed by our observations:

- It should be monotonic with respect to time.
- It should be negligible in the first hour or so of the experiment for all animals.
- It should either increase quickly and saturate, or increase slowly at first and continue accelerating until the end of the experiment.

To model these effects, we use a piecewise transfer function which modifies each  $\psi$  parameter as follows:

$$T_\psi(\psi, t) = \begin{cases} \psi, & \text{if } t \leq o_t \\ \psi + \vec{s}_t \odot \sigma(\vec{W}_t(t - \vec{o}_t) - 6) - I, & \text{otherwise} \end{cases} \quad (5)$$

where  $\odot$  denotes an element-wise product,  $\vec{s}_t$  is a set of trainable parameters which determines the maximum extent of the time degradation for each animal,  $\vec{W}_t$  determines the slope of the degradation, and  $\vec{o}_t$  contains a learned ‘onset’ value for each animal which determines when the time degradation begins.  $\sigma$  represents a sigmoid function ( $\sigma(x) = \frac{1}{1+e^{-x}}$ ) which scales the output between 0 and 1, and a fixed bias of -6 is added to ensure the result is close to zero when  $t = o_t$ .  $I$  is the ‘intercept’ given by  $I = \vec{s}_t \odot \sigma(-6)$  which must be subtracted to avoid a discontinuity at  $t = o_t$ .

Values of  $\vec{s}_t$  are constrained to be between 0 and 20, which keeps the scale of the time effects roughly equal to the original range of hearing loss encoded by the original  $\psi$  parameters (between -10 and 10). Values of  $\vec{W}_t$  are constrained to be between 0 and 50, which allows for both very slow and very rapid degradation and saturation, and  $\vec{o}_t$  is constrained between 0.05 and 0.5 - i.e. the onset of the effects must be between 30 minutes and 5 hours into the experiment.

## **Acknowledgements**

This work was supported by EPSRC EP/W004275/1 and BBSRC BB/Y008758/1. We also thank Prof. Maneesh Sahani for his helpful feedback.